Solar and Stellar Magnetic Fields: Origins and Manifestations
Proceedings IAU Symposium No. 354, 2019
A. Kosovichev, K. Strassmeier & M. Jardine, ed.
doi:10.1017/S1743921320000393

Examining the optical intensity and magnetic field expansion factor in the open magnetic field regions associated with coronal holes

Chia-Hsien Lin[1], Guan-Han Huang[1] and Lou-Chuang Lee[2]

[1]Graduate Institute of Space Science, National Central University, Taiwan
email: chlin@jupiter.ss.ncu.edu.tw

[2]Institute of Earth Sciences, Academia Sinica, Taiwan

Abstract. Coronal holes can be identified as the darkest regions in EUV or soft X-ray images with predominantly unipolar magnetic fields (LIRs) or as the regions with open magnetic fields (OMF). Our study reveals that only 12% of OMF regions are coincident with LIRs. The aim of this study is to investigate the conditions that affect the EUV intensity of OMF regions. Our results indicate that the EUV intensity and the magnetic field expansion factor of the OMF regions are weakly positively correlated when plotted in logarithmic scale, and that the bright OMF regions are likely to locate inside or next to the regions with closed field lines. We empirically determined a linear relationship between the expansion factor and the EUV intensity. The relationship is demonstrated to improve the consistency from 12% to 23%. The results have been published in Astrophysical Journal (Huang *et al.* 2019).

Keywords. magnetic fields, Sun: corona, Sun: magnetic fields, methods: statistical

1. Introduction

Coronal holes are major source regions of high speed solar wind streams, and their magnetic fields are the largest scale solar magnetic fields. Therefore, accurate determination of the locations and areas of the coronal holes is important for space weather forecast and the study of solar cycle variation of solar magnetic fields.

Two commonly used methods to identify the on-disk coronal holes are to identify them as (1) the darkest regions in EUV images with predominantly unipolar magnetic fields, and (2) the regions with "open" magnetic fields, which are the fields with field lines extending far away from the Sun.

While some studies reported that the coronal holes identified by the two methods are statistically associated (e.g., Levin 1982; Obridko & Shelting 1989; Mogilevsky *et al.* 1997; Neugebauer *et al.* 1998; Obridko & Shelting 1999; Hayashi *et al.* 2016), others have shown significant differences between the two (e.g., Lowder *et al.* 2014, 2017; Linker *et al.* 2017). The aim of this study is to investigate the conditions leading to different brightness of OMF regions. We use the magnetic field expansion factor f_s (Wang & Sheeley 1990) to represent the structure of open magnetic field, and apply statistical analysis to examine the relationship between the expansion factor and the EUV intensity.

2. Identification of coronal holes

The AIA 193Å images and HMI line-of-sight magnetograms are used for the identification of low EUV intensity coronal holes (LIR_{193}), and the Wilcox Solar Observatory

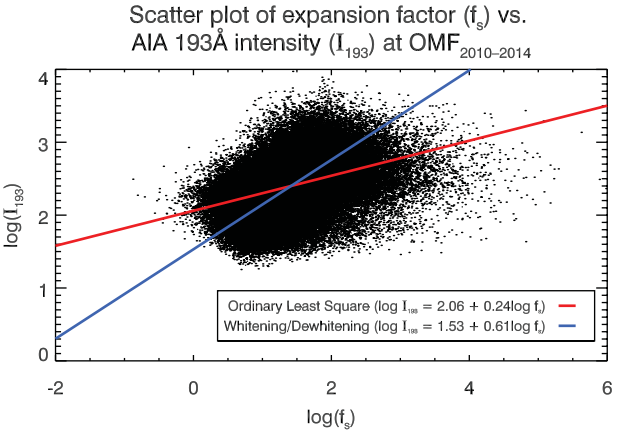

Figure 1. Scatter plot of expansion factor $\log f_s$ vs. AIA 193Å intensity I_{193}. The red and blue lines are the regression lines of using an OLS fit and WD transformation, respectively. (adapted from Huang *et al.* 2019)

radial-field synoptic maps are used for the identification of OMF coronal holes. To determine the LIR_{193}s, we first constructed synoptic maps of AIA images and HMI magnetograms, and identified LIR_{193}s from the maps based on a thresholding method developed by Krista & Gallagher (2009). To determine the OMF regions, we first applied Potential Field Source Surface (PFSS) model to construct 3D magnetic field between the solar surface and a upper boundary (source surface), and then identify the OMF regions as the footpoints of open magnetic field lines.

3. Statistical analysis

The statistical distribution profiles (histograms) of the expansion factor (f_s) and the intensity of AIA 193Å (I_{193}) show that both profiles are approximately log-normal, and that the shape of $\log f_s$ histogram changes with solar activity and latitude.

A scatter plot of $\log f_s$ vs. $\log I_{193}$, indicates a weak positive correlation between the two, with a correlation coefficient ≈0.39. To determine this linear relationship, we applied two linear regression methods: the ordinary least square (OLS) method and a regression method based on the concept of whitening/dewhitening (WD) transformation (Mayer *et al.* 2003). The best-fit OLS regression line is

$$\log I_{193} = 0.24 \log f_s + 2.05, \tag{3.1}$$

and the best-fit WD regression line is

$$\log I_{193} = 0.62 \log f_s + 1.51. \tag{3.2}$$

The scatter plot and the best-fit results of OLS and WD methods are presented in Figure 1 (adapted from Huang *et al.* 2019).

To evaluate the capability of using the OLS and WD regression lines to predict the brightness of an OMF region, we use Equations (3.1) and (3.2) to predict and extract the OMF regions with AIA 193Å intensities lower than the threshold used to identify the LIR_{193}coronal holes. The accuracy of OLS and WD predictions is quantified by computing the consistency level between the predictions and the LIR_{193} coronal holes:

$$C_{\mathrm{WD(OLS)}} \equiv \frac{\mathrm{LIR}_{\mathrm{WD(OLS)}} \cap \mathrm{LIR}_{193}}{\mathrm{LIR}_{\mathrm{WD(OLS)}}}, \tag{3.3}$$

https://doi.org/10.1017/S1743921320000393 Published online by Cambridge University Press

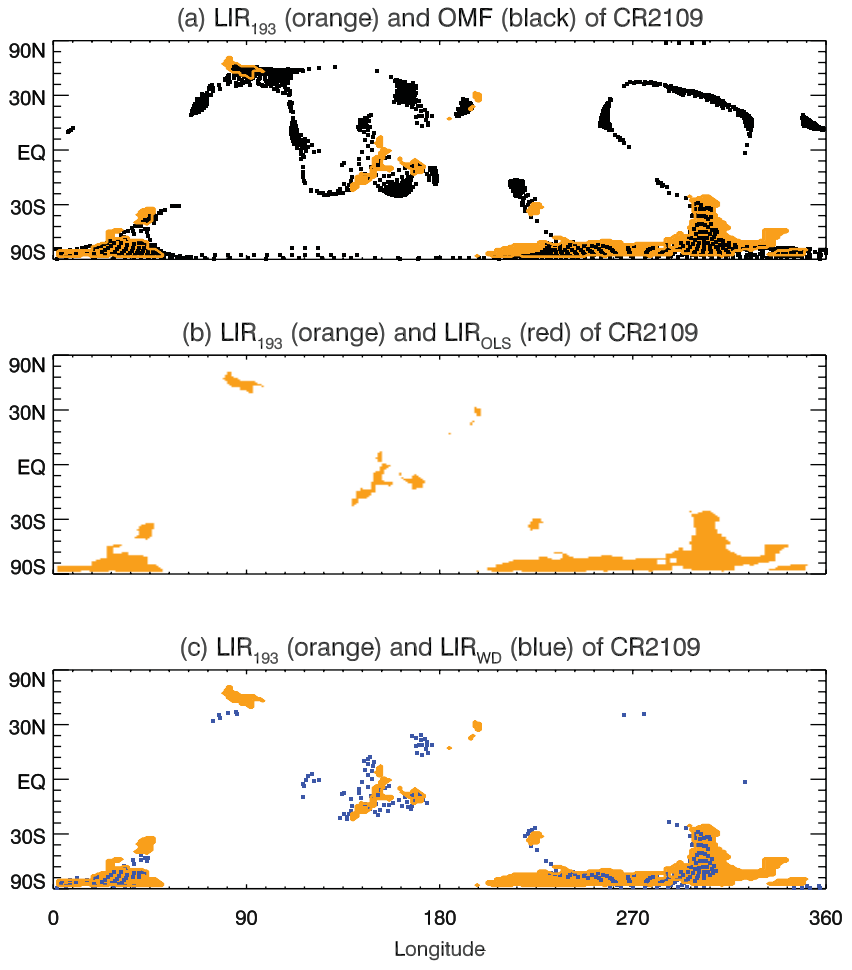

Figure 2. An example of comparison between AIA 193Å LIR_{193} (orange in all panels) and OMF, OLS-predicted low intensity regions (LIR_{OLS}, red in panel b), and WD-predicted low intensity regions (LIR_{WD}, blue in panel c). The selected synoptic map is CR2109. (adapted from Huang *et al.* 2019)

where $LIR_{WD(OLS)}$ are the WD-predicted (OLS-predicted) LIRs. The average consistency level for our data set 2010–2014 is 0.10 for OLS method and 0.23 for WD method. Comparing these with the consistency level between OMF and LIR_{193}, which is 0.12, we can see that while all three are not high, WD method clearly improved the average consistency level. Figure 2 shows an example of comparing LIR_{193} with LIR_{OLS} and LIR_{WD}. The plot shows that the WD regression line removed most of OMF regions that are inconsistent with LIR_{193} while keeping the OMF regions that conincide with LIR_{193}.

References

Hayashi, K., Yang, S., & Deng, Y. 2016, *JGRA*, 121, 1046
Huang, G.-H., Lin, C.-H., & Lee, L.-C. 2019, *ApJ*, 874, 45
Krista, L. D. & Gallagher, P. T. 2009, *Solar Physics*, 256, 87
Levine, R. H. 1982, *Solar Physics*, 79, 203
Linker, J. A., Caplan, R. M., Downs, C., *et al.* 2017, *ApJ*, 848, 70
Lowder, C., Qiu, J., & Leamon, R. 2017, *Solar Physics*, 292, 18

https://doi.org/10.1017/S1743921320000393 Published online by Cambridge University Press

Lowder, C., Qiu, J., Leamon, R., & Liu, Y. 2014, *ApJ*, 783, 142
Mayer, R., Bucholtz, F., & Scribner, D. 2003, *ITGRS*, 41, 1136
Mogilevsky, E. I., Obridko, V. N., & Shilova, N. S. 1997, *Solar Physics*, 176, 107
Neugebauer, M., Forsyth, R. J., Galvin, A. B., *et al.* 1998,*JGR*, 103, 14587
Obridko, V. N. & Shelting, B. D. 1989, *Solar Physics*, 124, 73
Obridko, V. N. & Shelting, B. D. 1999, *Solar Physics*, 187, 195
Wang, Y.-M. & Sheeley, N. R., Jr. 1990, *ApJ*, 355, 726

https://doi.org/10.1017/S1743921320000393 Published online by Cambridge University Press